2022 Second International Conference on Computer Science, Engineering and Applications (ICCSEA) | 978-1-6654-5834-4/22/$31.00 ©2022 IEEE | DOI: 10.1109/ICCSEA54677.2022.9936518

Methodological Analysis of Blood Pressure Learning using Boro Receptors Model

[1]Hemanta Kumar Bhuyan, [2]K. Sai Priya, [3]Kachihalli Milana
[1,2,3,]VFSTR University, Guntur, AP, INDIA
hmb.bhuyan@gmail.com
kondasaipriya7300@gmail.com
milanaanitha@gmail.com

Abstract: This paper addresses blood pressure learning with blood transfer and determination of high or low blood pressure (BP) as per the boro receptors model. Norepinephrine (NE) is commonly practiced for septic shock because it raises blood pressure. Blood pressure is critical for ensuring that BP ratio is fluctuating for septic patients which are appropriately controlled. Thus, this paper analyzes an arterial blood pressure framework for patients based on the receiving NE infusion in real-time physiology. We considered data learning methodologies frequently to treat the physiological consequences of septic shock patients. We considered different physiological parameters to predict the NE infusion rate. Our experiments got the root mean square error for mean arterial blood pressure prediction.

Index Terms— Mean arterial blood pressure (MAP), sepsis, least mean square, norepinephrine (NE), filter coefficient

I. INTRODUCTION

Blood pressure is a very sensitive chemical liquid flow in vein of human body that always helps to find out various diseases as per health information. We have analyzed this blood pressure in medical processes to find out various health information through our model. Severe infections are generated by patient's blood which are under fear of life. As we know, Sepsis-induced hypotension is treated with vasopressors such as epinephrine and norepinephrine (NE). NE is a useful vasopressor in the intensive care unit (ICU) for enhancing splanchnic tissue oxygen utilization [1]. To keep MAP levels as certain threshold, clinicians use their clinical judgment to adjust the pace of NE infusion. Patients with septic shock should have their MAP monitored constantly to ensure that the 65 mmHg criterion is met [2]. There should be regular reviews because NE's efficacy varies from patient to patient and with time [3,4]. Because of this, administering NE infusions is a time-consuming task in the clinic. Morbidity and death could result from human mistakes and inaccuracies in modifications.

To meet the needs of the medical community, a NE infusion rate-based MAP prediction system is in great demand. Because of this, an ICU data model that can reliably forecast MAP will be necessary for the development of such a system. Real-time adaptation to the changing physiology of a patient should be possible with these models. It is possible to forecast the future using a model based on physiological principles.

Machine learning frameworks have an data (sometimes known as "black boxes") explain ability issue when used in clinical contexts [5]. We have developed a time-varying, physiologically-informed modeling approach to accurately forecast the mean arterial pressure in patients with sepsis who are receiving nephroephedrine (NE) infusions.

Also, recent study [6] found that lowering blood pressure does not always mean restoring organ function. As a result, no reduction in mortality has been studied thus far. A machine learning model is used to better understand the NE response in septic patients and to create a methodology that is informed by physiology to forecast the MAP with more accuracy over the long run.

Various modeling strategies have been used to study arterial blood pressure prediction management. The infinite impulse response (IIR) adaptive filter was implemented by Koivo [7] and [8]. Arnsparger [9] employed an IIR adaptive model-based adaptive control system to manage blood pressure. Bhuyan et al., [10,14] considered deep learning and feature selection approach with biological data sets. The autoregressive-moving-average (ARMA) was then observed by researchers [11].

In recent research work, Su [12] and Li [13] developed recurrent neural networks to predict long-term blood pressure levels. As a result of this, neural networks require a large amount of training data to make accurate predictions. In the absence of appropriate data, these systems cannot be tailored to a single patient. Bhuyan et. al., developed the model for data extraction [24] and IoT based data analysis [25].

The baroreflex model was first proposed by Mukkamala [15], for analyzing blood pressure-related components working in the human body. A data-driven framework is not included in this model, although it is general enough to accommodate MAP prediction. Thus, the foundation of our physiology-based proposed framework is an expansion of this idea. We considered another model related to baroreflex model which is shown in fig 1.

We also used MAP model for Bororeflex. It's a black box model that doesn't take any specific physiological relationship into account, but the algorithm can accurately forecast the MAP value. As a result, it lacks a rational basis for explanation. In addition, because of its high processing cost, real-time implementation is difficult. While our method is more affordable and simpler to use than a fuzzy approaches, the connection it makes to a physiological model of NE in HR and PP may provide additional information. As a result, we evaluate the effectiveness of our approach against the alternatives. Our findings are also compared to autoregressive-moving-average with exogenous inputs (ARMAX) with an extension of the autoregressive-moving average (ARMA) model.

978-1-6654-5834-4/22/$31.00 ©2022 IEEE

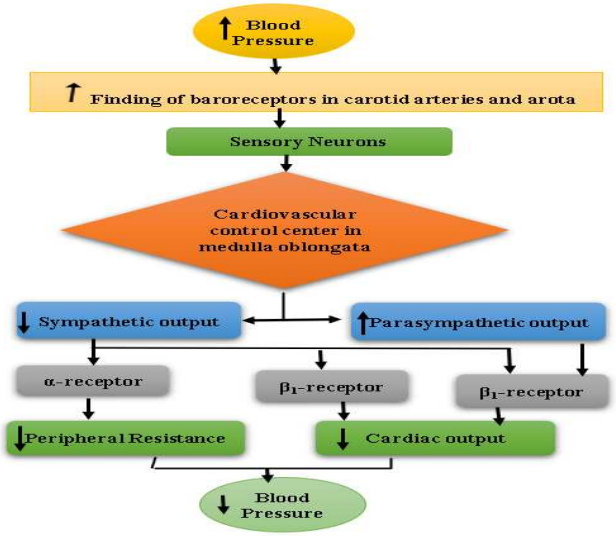

Fig. 1: Bororeflex with boro receptors model for blood pressure

Remaining sections of this paper are arranged as follows. We explained the proposed framework of NE-MAP model in section II. The methodologies of the proposed model are elaborated in section III. The experiments are demonstrated as per model and methodologies in section IV. We concluded our paper in section V.

II. FRAMEWORK OF PHYSIOLOGICAL NE-MAP MODEL FOR BLOOD PRESSURE

For our model, we use the principles of physiology NE MAP model. Because each patient's physiology changes over time and is unique, we build a 2-level model of MAP. Future heart HR, PP, and total KR are predicted by the first layer using data from the previous layer and the previous NE. To keep up with the changing health status of the patient, these models constantly modify and retrain themselves. In the second layer, physiology is used to forecast future MAP based on expected HR, PP, and KR. We have explained various methodology behind our physiology-based MAP model, as well as the steps involved in preparing the data for MAP prediction.

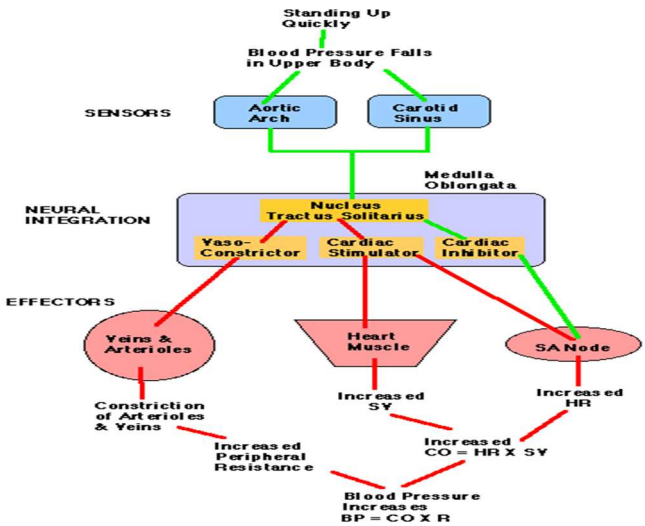

Fig 2: Various components of baroreceptor reflex for blood pressure

The human body's fast response system to variations in blood pressure is called the baroreceptor reflex. Inhibitory effects are depicted in green, while excitatory effects are shown in red. We designed baroreceptor reflex for blood pressure as in fig. 2 with various components such as (a) Sensors, (b) Neural integration, (c) Effectors as follows.

(a) Sensors: In the arteries of the upper body, pressure sensors are placed as:

1. React to blood pressure-induced stretching
2. There are fewer nerve impulses/sec in the Carotid sinus than there are in the rest of the body because blood pressure is higher (glossopharyngeal)
3. Carotid sinus: Sensory nerve = cranial nerve IX (glossopharyngeal)
4. Aortic arch: Sensory nerve = cranial nerve X (vagus)

(b) Neural Integration: Centers used to lower blood pressure include: the brain's nucleus tractus solitarius, which receives sensory neurons, and the medulla oblongata, where measurements of blood pressure are compared to a predetermined value (the "set point"). Increases heart output by activating the cardiac accelerator nerve as:

1. Uses the vagus nerve as a means of decreasing cardiac output.
2. arterioles and veins are constricted by the vasoconstrictor centre, which employs spinal neurons.
3. Flow resistance is increased when blood arteries are constricted (R)

(c) Effectors:

(i) Heart:

(i) SA Node: regulates the heartbeat rate (HR)

1. The vagus nerve slows the heart.
2. Cardiac accelerator increases the rate of heartbeats

(ii) Heart muscle:

1. SV (stroke volume) is controlled by the heart muscle and the cardiac accelerator nerve.
2. The cardiac muscle does not get any vagus fibres.

(ii) Arteries and Veins system

(d) Analysis of bood pressure

1. When blood pressure is low, the heart's ability to pump blood will be increased, and the arterioles and veins that carry blood through the body will be constricting. (CO = HR X SV) (Here, CO is cardiac output)
2. When blood pressure is high: Reflex decreases CO if pressure is high.
3. Arterioles and veins dilate as a result of decreased reflex activity arterial blood pressure (iii) Reflex will bring your blood pressure back to normal.

III. THEORETICAL ANALYSIS FOR PHYSIOLOGICAL MODEL

978-1-6654-5834-4/22/$31.00 ©2022 IEEE

We considered various mathematical formulas to analyze the blood pressure using physiological model. We used Wind Kessel model [19] to include parameters that can be measured in most ICUs patient. Based on a physiological model, we can predict MAP using HR, PP, and KR. Starting with [20], we considered various methods as per the model and made relationships among different components as follows.
We formulated the eq. (1) as

$$MAP = CO * Resist \quad (1)$$

Here, we considered Resist as a vascular resistance and CO as cardiac output. Each component of right-hand side of eq. 1 is defined again as eq 2 and 3 as follows.

$$CO = SV * HR \quad (2)$$

Here, SV is stroke volume. Pulse pressure (PP) also influences stroke volume, as it varies depending on systolic (SBP) and diastolic blood pressure (DBP) with differences. This is how we can express the stroke volume:

$$SV = k * PP = k * (SBP - DBP) \quad (3)$$

Where, k is a scalar coefficient. The eq. (1) is further derived using eq.(2) and (3) and got eq. (4) as follows

$$MAP = (SBP - DBP) * HR * K * Resist \quad (4)$$

$$KR_o = k * Resist \frac{A_d}{P_s - DBP - P_0} \quad (5)$$

A_d determines the area of the arterial blood pressure (ABP) curve, P_s is the dicrotic pressure, and P_0 is the downstream pressure arterial model.
It is recommended by Chemla [21] that P_0 be a small integer that changes slowly over time. The MAP can be stated by swapping (5) for (4).

$$MAP = (SBP - DBP) \times HR \times \frac{A_d}{P_s - DBP - P_0} \quad (6)$$
$$= PP \times HR \times KR_0$$

Since the MAP may be calculated as the product of three different measurements, the eq. (6) is formulated as per measurements such as PP = pulse pressure; HR = heart rate; TAC = total artery compliance; and R = arterial resistance (KR_0). P_0 is an unknown parameter in (6) and measurement of the P_0 is difficult in the current clinical setting. We can however, (6) using a linear model because the value is tiny and slowly varying.

$$MAP \approx S \times PP \times HR \times KR + c \quad (7)$$

where KR $= \frac{A_d}{P_s - DBP}$, , s and c two factors for scaling factor and offset respectively which are determined by linear regression.

We considered that each of these variables changes based on its previous values and on previous NE injection rates as well. As per present and previous PP, HR, KR, and NE values, we can therefore conclude that future values can be predicted.

A. Least Mean Square (LMS) Model

Based on the preprocessed data, we used above model and learn through PP, HR and KR components. We used a 2-stage procedure to discover the association among prior and present values. The association between each of the parameters and NE is specifically determined as follows:

$$y[n] = \sum_{a=1}^{N} \alpha_a[n] y[n - a - P] + \sum_{b=0}^{N} \beta_b[n] x[n - b - P] \quad (8)$$

Here, y[n] is formulated in as per above 3- items for time and the NE input is x[n] in that order. We use a normalized LMS approach to learning the coefficients on various time as $\alpha_a[n]$ and $\beta_b[n]$. The weights w[n] in this model are continuously updated as a result of the model learning and adapting to

$$w[n] = w[n-1] + \frac{\mu e[n]}{0.001 + u[n]u^T[n]} u[n] \quad (9)$$

Here, w[n] is determined with the help of parameters $\alpha_a[n]$ and $\beta_b[n]$ as below. The u[n] matrix is defined as eq. (10) as

$$w[n] = [\alpha[n]\beta[n]] = [\alpha_1[n] \dots \alpha_N[n]\beta_0[n] \dots \beta_N[n]]$$
$$u[n] = [y[n]x[n]] = [y[n] \dots y[n-N]x[n] \dots x[n-N]] \quad (10)$$

From eq. (9), the value 0.001 is used to alleviate the system based on avoiding zero from denominator. As per above equation the error e[n] is determined as:

$$e[n] = y[n] - w[n]u^T[n] \quad (11)$$

B. Associative Learning with the Physiological components

The linear algebra is developed using various components (PP, HR, and KR) and MAP and formulated the eq. (12) as follows.

$$MAP[n] = s[n](PP[n] \times HR[n] \times KR[n]) + c[n] \quad (12)$$
$$= [s[n]c[n]].\begin{bmatrix} PP[n] \times HR[n] \times KR[n] \\ 1 \end{bmatrix}$$

Here s[n] and c[n] are scale and offset coefficients respectively which is further defined as eq. (13).

$$[S[n]c[n]] = MAP[\begin{matrix} PP[n] \odot HR[n] \odot KR[n] \\ 1 \end{matrix}]^{\dagger}$$
$$[s[n]c[n]] = MAP[n] \begin{bmatrix} PP[n] \odot HR[n].KR[n] \\ 1 \end{bmatrix}^{\dagger} \quad (13)$$

Where $[\cdot]\dagger$ represents pseudo-inverse operation and $\odot$ identify the entry wise product.

C. Prediction of the Model

The assumption is taken based on the relationship between past and current data of P time sample. It is therefore possible

978-1-6654-5834-4/22/$31.00 ©2022 IEEE

to forecast future data using the training weights (a and b) from (8). To be more specific, we use computation to forecast the three future components of HR, PP, and KR.

$$y[n+p] = \sum_{a=1}^{N} \alpha_a [n] y[n-a] + \sum_{b=0}^{N} \beta_b [n] x[n-b] \quad (14)$$

where y[n] is defined on above components and expected MAP is defined by

$$MAP[n+P] = s[n](PP[n+P] \times HR[n+P] \times KR[n+P]) + c[n] \quad (15)$$

With the help of s[n] and c[n] from (13), eq. (15) is formulated.

D. Comparison methods

Different feedback for filter coefficient are used such as coefficient for the exogenous input NE, and a coefficient for white noise. Modelling future MAP with this method involves filtering out the prior iteration of each component (past NE and MAP), then creating a stationary white noise process. However, this model just links future MAP to the NE, which is comparable to our model. Each future HP, PP, and KR in turn is linked with NE in our method before being connected to MAP in the present.

We considered three alternative adaptive models for comparing to our approach such as ARMAX model [17], an IIR linear model [18], and least squares regression approach [4]. We used the IIR and ARMAX models as their time-series forecasting. Thus, the data in the ARMAX model is assumed to be

$$MAP[n] = \sum_{\alpha=1}^{N} \varphi_\alpha MAP[n-\alpha] + \sum_{b=1}^{N} \theta_b NE[n-b] \dots\dots\dots + \sum_{c=1}^{N} \eta_c \varepsilon[n-c] \quad (16)$$

where ϕ_a, θ_b and θ_c are different feedback for filter coefficients, the exogenous input NE, and coefficient for white noise ε respectively.

Again, the IIR method is formulated as

$$MAP[n+P] = \sum_{a=0}^{N} \varphi_a MAP[n-a] + \sum_{b=1}^{N} \theta_b NE[n-b] \quad (17)$$

Based on our methodology, IIR filter model y[n] is used in both equations (17) and (8) to derive the MAP values. A normalized LMS method is used to solve this model, just like in (9). Assume that w[n] and u[n] are the weights in this case. We defined two vectors such as w[n] and the u[n] as follows.

$$w[n] = [\emptyset[n]\theta[n]] = [\varphi_{1 \dots\dots \varphi_N} \theta_{1 \dots \theta_N}]$$
$$u[n] = [NE[n]MAP[n]]$$
$$= [NE[n] \dots NE[n-N]MAP[n] \dots MAP[n-N] \quad (18)$$

There are several similarities between the ARMAX and IIR versions. The MAP model uses this term to describe unpredictability. LMS is a common algorithm used in both the IIR model and our model.

More information can be found in [4]. Despite its effectiveness, our previous method requires extensive computation and lacks clarity. We used black-box models with limited physiological explanation in all three comparisons.

IV. EXPERIMENTS AND ITS ANALYSIS

A. Data set

To ensure that our procedure is accurate, we use two sources of patient data. The Research Data Export (RDE) functionality of Philips Intellivue monitors is used to gather data for the Intermountain Medical Center [16]. Once a minute, the NE is injected into the body. All of the heart's electrical activity is recorded and output at a steady frequency of 125 hertz until the next cardiac cycle. We subsequently reduced the sampling rate to 5 Hz to speed up the calculation.

Because 51 individuals had fewer than two hours of unbroken ABP signals or were physically moving, 82 of the 103 patients' data was removed. Thirty-one more individuals are either unaware of NE or are taking several vasopressors. The only vasopressor treatment given to each of the 21 patients is NE for 2-24 hours.

Using three different vantage points, we explore the predictions made by our model in this part. We explain other approaches for forecasting future MAPs, and we compare our predicted accuracy to those of these other methods. For real-time forecasting, we must also take into account the processing cost. It shows the explain ability of our method's adaptive filter coefficients.

B. Computational Output

Here, we examine each method's ability to predict MAP accurately. We assess accuracy by calculating the root mean square error (RMSE) between the observed and forecasted MAP values. To determine how far ahead we can forecast MAP, we use a range of prediction times ranging from 3.33 minutes to 20 minutes. The timer is set to 3.33 minutes for ease of use. For a sampling rate of 5Hz, this time corresponds to around 1000 samples.

Noise and the interaction between sympathetic and parasympathetic nervous systems may be responsible for the 0.001Hz to 0.01Hz oscillations in MAP measured in this study [22]. Our model does not include this part of MAP. That's why we don't keep a record of it. However, additional information may be necessary before this information can be included.

Our proposed model is compared to another model as in Table I. More than 8.5 mmHg is forecasting, and it reaches 10 mmHg at 10 minutes. As a result, in Table I, ARMAX is omitted. A MAP inaccuracy of less than 5 mmHg is preferred to maintain the patient's continued good health. To put it another way, our method is more efficient than the reduction rank least squares model and IIR model in terms of effective prediction time.

Table I: RMSE of MAP prediction with prediction time

	Mean MAP Error		
Prediction Time	Our Method	IIR Model	Reduced rank mean squares
3	3.5	3.5	3.0

978-1-6654-5834-4/22/$31.00 ©2022 IEEE

6.2	4.2	4.3	4.1
10	4.9	5.9	5.3
13.8	5.0	7.5	6.1
17	5.8	10.2	7.0
20	6.2	13.2	7.9

As shown in Table I, multiple comparisons are carried out after a well-balanced one- and two-way analysis of variance. Using the two-way ANOVA p-value of 2.88e-8 in the last column of Table II, we can conclude that the RMSE forecasts of the three approaches differ significantly. When the prediction time is greater than 6.67 minutes, the p-value drops below 0.05. When the prediction duration is longer than 6.67 minutes, the prediction RMSE of the three approaches may be separated.

C. Computational Cost

In our models, the data memory length is equal to N. Table II shows how much each approach costs to compute concerning the amount of RAM available. This prediction process would be run in our system at 0.2 sec.

In comparison to the IIR approach, our model is just five times as sluggish. Thus, the ARMAX method's processing time exceeds the sample period by more than 0.2 seconds.

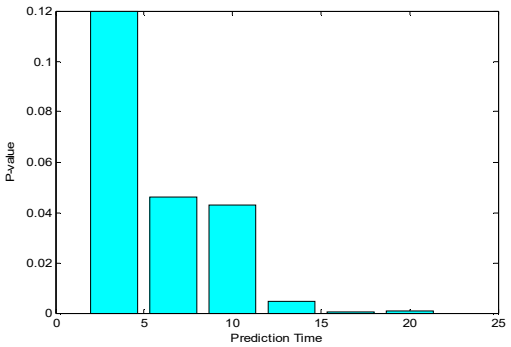

Fig. 3: ANOVA Results For RMSE IN 3 Methods

Table II shows that the IIR model, which is the speed up and has the worst accuracy. To accurately forecast HR, PP, and KR, our model makes use of three different IIR models (three times the computational cost). An additional computational cost of around five times that of the IIR model is incurred when the three forecasts are combined using a 3N by 2 matrices [4].

Table II: The computational cost compare with different model

Data Memory size (Minutes)	IR Model	Our Model	Reduced Rank Least Square	AR Max
2	10^{-4}	$10^{-3.2}$	$10^{-1.8}$	$10^{-0.2}$
4	$10^{-3.9}$	$10^{-3.1}$	$10^{-1.7}$	$10^{-0.19375}$
6	$10^{-3.8}$	$10^{-3.0}$	$10^{-1.65}$	$10^{-0.1875}$
8	$10^{-3.72}$	$10^{-2.9}$	$10^{-1.64}$	$10^{-0.175}$
10	$10^{-3.68}$	$10^{-2.8}$	$10^{-1.63}$	$10^{-0.1625}$
12	$10^{-3.6}$	$10^{-2.7}$	$10^{-1.62}$	$10^{-0.15}$
14	$10^{-3.55}$	$10^{-2.6}$	$10^{-1.61}$	$10^{-0.1375}$
16	$10^{-3.52}$	$10^{-2.5}$	$10^{-1.6}$	$10^{-0.125}$
18	$10^{-3.52}$	$10^{-2.4}$	$10^{-1.59}$	10^{-1125}
20	$10^{-3.51}$	$10^{-2.3}$	$10^{-1.5}$	$10^{-0.1062.5}$
22	$10^{-3.5}$	$10^{-2.33}$	$10^{-1.4}$	$10^{-0.10625}$
24	$10^{-3.5}$	$10^{-2.4}$	$10^{-1.3}$	$10^{-0.1}$

In the end, ARMAX is the most sluggish than others as in table II. Iteratively repeating the all process till the prediction time is achieved will be necessary for the system to anticipate more than one future sample.

D. Coefficients of the NE filter

Furthermore, we may follow the filter coefficients, referred to in (9), for each physiological component using our model. However, It is important to note that our model coefficients do not just fluctuate with time but also vary between patients. It is important to note that the effects of NE vary depending on the type of patient and their current health situation. For HR and PP, we observed that the coefficients have similar behavior. Slower effects diminish for some individuals, such as patient 1, then for others, such as patient 2.

KR operates differently than HR and PP. During the 14-minute mark, patient 1 responds the most, while patient 2 responds the least. Compared to HR and PP, KR exhibits a far greater degree of variability among patients. In general, the KR coefficients are much greater (by a factor of more than ten times) than the HR and PP coefficients.

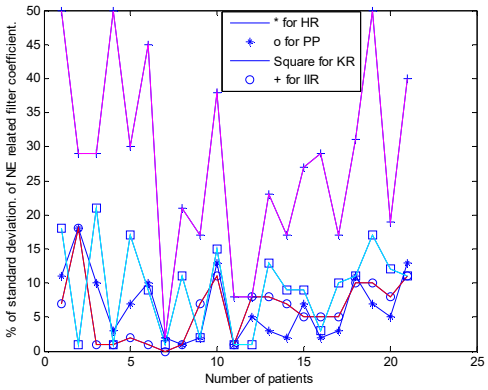

Fig. 4: Percentage of Standard Deviation of NE with different components

There are the two components that makeup KR, and NE has been shown to have a significant impact on total peripheral resistance [23]. Different coefficient components related to NE are shown in Fig. 4. To illustrate the NE-MAP relationship, we depict the filter coefficients' standard deviations from the IIR filter. In general, Different components with NE for the vast majority of patients have relative standard deviations between

978-1-6654-5834-4/22/$31.00 ©2022 IEEE

2% and 20%. The IIR coefficients/NE-MAP coefficients have much higher relative standard deviations.

The HR filter coefficients (P-value 0.01) are substantially linked with the PP filter coefficients. The mean filter coefficients for 21 patients at the Intermountain Medical Center are negatively correlated. The PP response coefficients are also quite high. NE has a marginally greater impact on PP than HR. Since the average filter coefficients are modest, this shows that the patient's PP is not affected as much by NE as compare to another model. Our prediction has a 12-point range Vasopressors like NE, which are included in the calculation, increase this range by a factor of at least four-point.

V. CONCLUSIONS

The MAP modelling is considered with NE infusion to test individual sepsis patient in this work. We were able to develop a new MAP prediction model using data from the ICU. Two different databases were cross-validated using time series cross-validation. Our methods outperform three other proposed methods in terms of accuracy. In addition, the computing burden on our system is kept to a minimum. The learned filter coefficients also differ between patients, as we proposed. Since our method uses fewer computations, its accuracy is more than other approaches with less computational cost. A new approach for predicting the MAP in septic patients who are receiving NE as a vasopressor. In the future, we plan to use strong machine learning approach for arterial blood pressure model.

REFERENCES

[1] P. E. Marik and M. Mohedin, "The contrasting effects of dopamine and norepinephrine on systemic and splanchnic oxygen utilization in hyperdynamic sepsis," *Jama*, vol. 272, no. 17, pp. 1354–1357, 1994.

[2] A. Rhodes *et al*., "Surviving sepsis campaign: international guidelines for management of sepsis and septic shock: 2016," *Intensive Care Medicine*, vol. 43, no. 3, pp. 304–377, 2017.

[3] H. Beloeil *et al.*, "Norepinephrine kinetics and dynamics in septic shock and trauma patients," *Brit. J. Anaesthesia*, vol. 95, no. 6, pp. 782–788, 2005.

[4] Y. Tang *et al.*, "Reduced rank least squares for real-time short term estimation of mean arterial blood pressure in septic patients receiving norepinephrine," *IEEE J. Translational Eng. Health Medicine*, vol. 7, pp. 1–9, Jun. 2019.

[5] A. Holzinger *et al.*, "What do we need to build explainable AI systems for the medical domain?" Dec. 2017, *arXiv:1712.09923*.

[6] M. Merouani *et al.*, "Norepinephrine weaning in septic shock patients by closed loop control based on fuzzy logic," *Critical Care*, vol. 12, no. 6, 2008, Paper R155.

[7] A. Koivo, D. Larnard, and R. Gray, "Digital control of mean arterial blood pressure in dogs by injecting a vasodilator drug," *Ann. Biomed. Eng.*, vol. 9, no. 3, pp. 185–197, 1981.

[8] A. J. Koivo, "Automatic continuous-time blood pressure control in dogs by means of hypotensive drug injection," *IEEE Trans. Biomed. Eng.*, vol. BME-27, no. 10, pp. 574–581, Oct. 1980.

[9] J. M. Arnsparger *et al.*, "Adaptive control of blood pressure," *IEEE Trans. Biomed. Eng.*, vol. BME-30, no. 3, pp. 168–176, Mar. 1983.

[10] Bhuyan H. K., Ravi V. K., Analysis of Sub-feature for Classification in Data Mining, IEEE Transaction on Engineering Management, 2021 (Early Published).

[11] S. Lu, K. H. Ju, and K. H. Chon, "A new algorithm for linear and nonlinear arma model parameter estimation using affine geometry [and application to blood flow/pressure data]," *IEEE Trans. Biomed. Eng.*, vol. 48, no. 10, pp. 1116–1124, Oct. 2001.

[12] P. Su *et al.*, "Long-term blood pressure prediction with deep recurrent neural networks," in *Proc. IEEE EMBS Int. Conf. Biomed. Health Informat.*, 2018, pp. 323–328.

[13] X. Li, S.Wu, andL.Wang, "Blood pressure prediction via recurrent models with contextual layer," in *Proc. 26th Int. Conf. World Wide Web*, 2017, pp. 685–693.

[14] Bhuyan H. K., Chakraborty C, Shelke Y, Pani S. K., COVID-19 diagnosis system by deep learning approaches, Expert Systems, Vol 39, Issue 3, pp. 1-18, July 2021. (Early Published).

[15] R. Mukkamala and R. J. Cohen, "A forward model-based validation of cardiovascular system identification," *Amer. J. Physiol.-Heart Circulatory Physiol.*, vol. 281, no. 6, pp. H2714–H2730, 2001.

[16] A. E. Johnson *et al.*, "Mimic-iii, a freely accessible critical care database," *Scientific Data*, vol. 3, 2016, Art. no. 160035.

[17] E. J. Hannan, *Multiple Time Series*, vol. 38, Hoboken, NJ, USA: Wiley, 2009.

[18] P. Regalia, *Adaptive IIR Filtering in Signal Processing and Control*. Evanston, IL, USA: Routledge, 2018.

[19] F. Otto, "Die grundform des arteriellen pulses," *Zeitung Fur Biologie*, vol. 37, pp. 483–586, 1899.

[20] M. N. Levy *et al.*, *Cardiovascular Physiol.*. St. Louis, MO, USA: Mosby, 2007, vol. 146.

[21] D. Chemla *et al.*,"Total arterial compliance estimated by stroke volume-toaortic pulse pressure ratio in humans," *Amer. J. Physiol.-Heart Circulatory Physiol.*, vol. 274, no. 2, pp. H500–H505, 1998.

[22] P. B. Persson *et al.*, "Identification of major slow blood pressure oscillations in conscious dogs," *Amer. J. Physiol.-Heart Circulatory Physiol.*, vol. 259, no. 4, pp. H1050–H1055, 1990.

[23] D. S. Goldstein *et al.*, "Relationship between plasma norepinephrine and sympathetic neural activity." *Hypertension*, vol. 5, no. 4, pp. 552–559, 1983.

[24] Bhuyan H. K. and Chakraborty C., Explainable Machine Learning for Data Extraction Across Computational Social System, Ieee Transactions On Computational Social Systems, April 2022. (Early Access)

[25] Chakraborty C, Mishra K, Majhi S. K., Bhuyan H. K., Intelligent Latency-aware tasks prioritization and offloading strategy in Distributed Fog-Cloud of Things, May 2022. (Early Access)

978-1-6654-5834-4/22/$31.00 ©2022 IEEE